Turkish Journal of Electrical Engineering & Computer Sciences

http://journals.tubitak.gov.tr/elektrik/

Research Article

Turk J Elec Eng & Comp Sci
(2017) 25: 3468 – 3474

doi:10.3906/elk-1604-360

Relaxation rate and polarization charge density model for AlN/Al$_x$Ga$_{1-x}$N/AlN heterostructures

Nagarajan SIVARAJAN[1,*], **Reeba KORAH**[2], **Maria Kalavathy GNANAMANI**[3]
[1]Department of Electronics and Communication Engineering, S.K.P. Engineering College, Tiruvannamalai, India
[2]Department of Electronics and Communication Engineering, Alliance University, Bengaluru, India
[3]Department of Computer Science and Engineering, St. Joseph's College of Engineering, Chennai, India

Received: 26.04.2016 • **Accepted/Published Online:** 06.02.2017 • **Final Version:** 30.07.2017

Abstract: This work describes the strain-relaxation–dependent carrier concentration (n_s) profile model using spontaneous and piezoelectric polarization for AlN/Al$_x$Ga$_{1-x}$N/AlN HEMTs in all mole fraction (x) interpolations. As x varies, the Aluminum Gallium Nitride (AlGaN) channel shows strain relaxation with the Aluminum Nitride (AlN) barrier. The degree of relaxation is modeled from AlN to GaN regions in the channel. It shows that the AlN barrier and buffer relaxation and strain recovery occurs due to the gradual crystal quality degradation from barrier/buffer to the channel interface. These combination devices show less drain current degradation with temperature variation from 300 K to 573 K. This model shows a good agreement with experimental data with a carrier density of $n_s = 2.8 \times 10^{13}/\text{cm}^2$.

Key words: AlGaN channel, sheet carrier concentration model, Ga-face, polarization, high breakdown, total induced net interface polarization

1. Introduction

For next-generation power devices, III–V nitride compound semiconductor devices have proven to be a promising candidate because of their attractive physical properties. Among these III–V devices, AlN- and GaN-based devices have demonstrated record high frequency (f_t) and high breakdown voltage (V$_{BO}$) [1–3]. Recently, AlN barriers have been incorporated in GaN-channel–enhanced device power characteristics like V$_{BO}$ and power density [4]. For Al$_{0.53}$Ga$_{0.47}$N/Al$_{0.38}$Ga$_{0.62}$N HEMT with gate-drain distances of 3 and 10 μm, V$_{BO}$ improved from 463 V to 1650 V [5]. Further increases in Al composition in the barrier and channel (Al$_{0.86}$Ga$_{0.14}$N/Al$_{0.51}$Ga$_{0.49}$N HEMT) increase source-to-drain V$_{BO}$ to 1800 V [6]. Thus, incorporating AlN in the barrier and the channel boosts device performance for high-power applications. Negligible drain current degradation (about 4%) is reported for a temperature increase from 300 K to 573 K during device operation with AlN/Al$_{0.60}$Ga$_{0.40}$N/AlN HEMT devices [7]. This degradation is significantly less than that of GaN-based devices because of the higher electron velocity of the AlGaN channel. Here a contact resistivity of $1.9 \times 10^{-2}\Omega$/cm is achieved with metal stack of Zr/Al/Mo/Au and by annealing at 950 °C. Moreover, the Al$_{0.31}$Ga$_{0.69}$N/Al$_{0.06}$Ga$_{0.94}$N/Al$_{0.06}$Ga$_{0.94}$N combination delivers an output power density of 4.5 W/mm with a power-added efficiency of 59% using the load pull measurement at a frequency of 4 GHz. In comparison with GaN HEMT devices, the figure of merit is less because of the higher alloy disorder scattering with higher Al combination in the channel and the barrier [8]. In reality, these devices with higher Al combination provide

*Correspondence: notoutnaga@gmail.com

better benchmarking for high-breakdown and high-temperature operation. Free-standing AlN substrate shows a best lattice match with AlN buffer and the dislocation degradation is less than 10^6 cm^{-2} in AlGaN/GaN HEMT devices [9]. The presence of an AlN back barrier with intrinsic AlGaN channel improves device threshold to +3 V, maintaining switching losses for low power applications. An Al mole fraction of 0.75 with AlN back barrier is suited for high-current as well as high-breakdown applications [10].

In this paper, the spontaneous and piezoelectric polarization model for an AlN/$Al_xGa_{1-x}N$/AlN HEMT device with mole fraction (x) interpolated from 0 to 1 is reported. Relaxation and strain recovery is observed in these devices due to the gradual degradation of crystal quality by varying x interpolation from 1 to 0. At $x = 0.3$, the lattice relaxation occurs, recovering crystal quality for a film thickness of 10 μm and repeats at $x = 0.7$ for 5 μm film thickness.

The paper is organized as follows: the introduction features a brief description about $Al_xGa_{1-x}N$ or AlN/$Al_xGa_{1-x}N$/AlN HEMT devices with an incremental effect of AlN interpolation in the barrier. Section 2 explores the device structure and Section 3 shows the polarization with the carrier density model in AlN/$Al_xGa_{1-x}N$/AlN HEMT devices. Finally, this device model is verified with experimental data.

2. Device description

Figure 1 shows the device cross section of a modeled AlGaN channel with an AlN buffer, barrier, and substrate. The unintentionally doped $Al_xGa_{1-x}N$ channel and AlN barrier are grown on AlN buffer at high temperature. The AlN buffer layer is essential to achieve a high-quality AlN channel. The channel and barrier thickness are 600 nm and 25 nm respectively, as per experimental paper dimensions [11]. The sheet carrier concentration from the Hall measurement at room temperature for AlN/$Al_{0.51}Ga_{0.49}N$/AlN HEMT is $2.8 \times 10^{13}/cm^2$. Source/drain regions are heavily doped and ohmic regions are formed. The contact resistance is derived from the ohmic contact interfaces. For the polarization model, only 2DEG formed at the AlN/AlGaN interface is considered in the calculations and hence it is assumed that the barrier region is completely ionized and that all the carriers are accumulated at the interface. Only the Gallium (Ga) face is considered for calculation of the carrier density model.

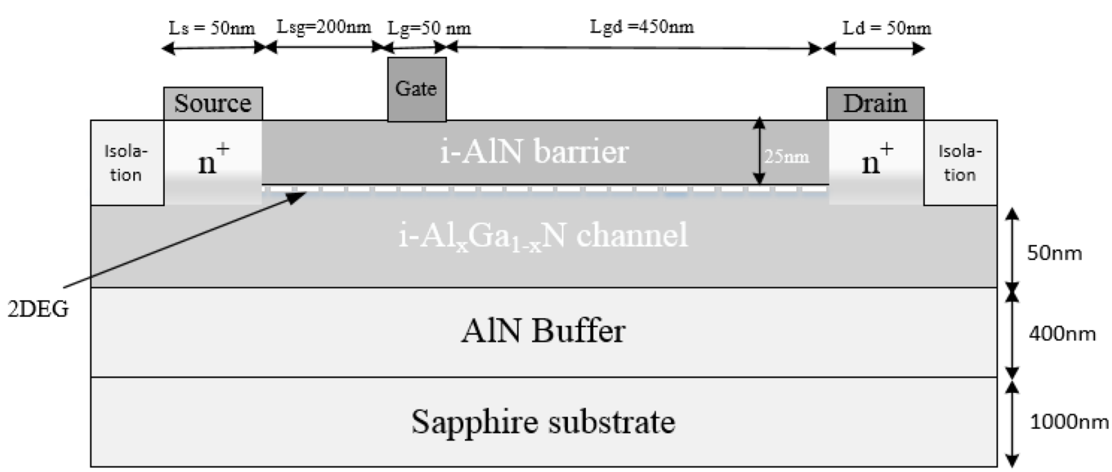

Figure 1. Device structure for AlN/$Al_xGa_{1-x}N$/AlN HEMT devices with x varied from 1 to 0.

3. Polarization and sheet charge density

In this work, the AlN/AlGaN region is assumed as the Ga face. The elastic constants used for the model are denoted by c_{33} and c_{11}. Polarization parameters are taken from [11]. The total polarization induced by piezoelectric polarization at the AlGaN/AlN interface is given by

$$\left\{ \begin{array}{l} c_{13}\_AlGaN = (5x + 103)Gpa \\ c_{33}\_AlGaN = (-32x + 405)Gpa \\ c_{13}\_AlN = 108Gpa \\ c_{33}\_AlN = 373Gpa \end{array} \right\} \tag{1}$$

The lattice constant parameters for barrier and channel regions are given by

$$\left\{ \begin{array}{l} a\_AlGaN = (3.189 - 0.077x)10^{-10}m \\ a\_AlN = (3.112)10^{-10}m \end{array} \right\} \tag{2}$$

The piezoelectric constants for the above AlGaN/AlN interface are

$$\left\{ \begin{array}{l} e_{31}\_AlGaN = (-0.11x - 0.49)C/m^2 \\ e_{33}\_AlGaN = (0.73x + 0.73)C/m^2 \\ e_{31}\_AlN = -0.64C/m^2 \\ e_{33}\_AlN = 1.46C/m^2 \end{array} \right\} \tag{3}$$

The spontaneous polarization and the total spontaneous polarization are given by

$$\left\{ \begin{array}{l} Psp\_AlGaN = (-0.052x - 0.029)C/m^2 \\ Psp\_AlN = -0.081C/m^2 \end{array} \right\} \tag{4}$$

$$P_{sp,total} = [Psp\_AlN - Psp\_AlGaN]$$

4. Relaxation rate and piezoelectric polarization

The piezoelectric polarization is reduced as the Al composition increases due to the strain relaxation in GaN channel heterostructures. In this device, strain relaxation is analyzed for a barrier thickness of 25 nm. As the alloy composition of x in the channel is varied from 1 to 0, the barrier is completely relaxed with the channel region. Let $r\ (x)$ be the relaxation rate for all interpolation ranges. The model used to define the relaxation rate is given by

$$\gamma = \frac{a\_AlGaN - a\_AlN}{a\_AlGaN^{(0)} - a\_AlN^{(0)}}; \tag{5}$$

here a_AlGaN and a_AlN are the inplane lattice constants measured for AlGaN channel and AlN barrier regions. The lattice constants a_AlGaN(0) and a_AlN(0) are in plane at zero strain from Eq. (2).

The relaxation rate assumed model from carrier density is given by

$$\gamma = \left\{ \begin{array}{ll} 0 & 0 < x < 0.2 \\ 0.5x + 0.20 & 0.5 < x < 75 \\ 1 & 0.75 < x < 1 \end{array} \right\} \tag{6}$$

The piezoelectric polarization is calculated by the difference between AlN and AlGaN piezoelectric charge density as follows:

$$Ppz = -2(1 - relaxationrate)strain \begin{bmatrix} \left[e_{31}\_AlN - \frac{e_{33}\_AlN.c_{13}\_AlN}{c_{33}\_AlN}\right] \\ -\left[e_{31}\_AlGaN - \frac{e_{33}\_AlGaN.c_{13}\_AlGaN}{c_{33}\_AlGaN}\right] \end{bmatrix} \tag{7}$$

The total polarization confined charge by spontaneous and piezoelectric polarization is given by

$$\sigma(x) = [Psp + Ppz]; \tag{8}$$

5. Carrier density model

Total carrier density depends upon the difference between the total charge induced by spontaneous and piezoelectric polarization and the Fermi energy level position in the potential well. The carrier density model and the parameters are

$$n(x) = \frac{\sigma(x)}{e} - \left(\frac{\varepsilon_0\varepsilon(x)}{d\_AlGaN.e^2}\right)(e\Phi_b(x) + E_f(x) - \Delta E_c); \tag{9}$$

here $\sigma(x)$ represents the total polarization charge, $\varepsilon(x)$ is the dielectric constant, e is charge of electrons, d_AlGaN is the thickness of AlGaN barrier, $e\Phi_b(x)$ represents the Schottky barrier of AlGaN and gate interface, $E_f(x)$ is the Fermi level, and ΔE_c represents conduction band discontinuity.

The band gap and conduction band offsets are given by

$$\begin{cases} E_g(AlN) = 6.13; \\ E_g(GaN) = 3.42; \\ E_g(AlGaN) = xE_g(AlN) + (1-x)E_g(GaN) - x(1-x)1.0eV; \\ \Delta E_c = 0.7[E_g(AlN) - E_g(AlGaN)]; \end{cases} \tag{10}$$

6. Results and discussion

The experimental results and proposed model show excellent concurrence for predicting sheet carrier concentration characteristics of AlGaN channel with AlN barrier with respect to different material compositions. The device is simulated using Sentaurus TCAD simulation (Synopsys; Mountain View, CA, USA). The density gradient mode along with carrier confinement is included to match the experimental data.

Figure 2 shows the spontaneous polarization charge for AlN/$Al_xGa_{1-x}N$/AlN HEMT with all x interpolations from 1 (AlN) to 0 (GaN). Constant barrier thickness is assumed as 25 nm. The total polarization charge (spontaneous and piezoelectric polarization) as a function of Al mole fraction is shown in Figure 3. As the Al mole fraction is decreased, the total polarization charge increases. As x is varied from AlN to GaN in the channel, it relaxes with the barrier and the piezoelectric charge is confined in 2DEG (Figure 3).

Total confined 2DEG charge due to spontaneous and piezoelectric polarization is analyzed in Figure 4. Spontaneous and piezoelectric charge increases when the band difference increases between the barrier and channel (Figure 4). Incorporation of the carrier density model in spontaneous and piezoelectric polarization analyzed from Eq. (9) is plotted in Figure 5. As the channel varies from AlN to GaN, the confined sheet charge density increases with the barrier thickness. The effects of Fermi level and conduction band discontinuity are incorporated using Eq. (10).

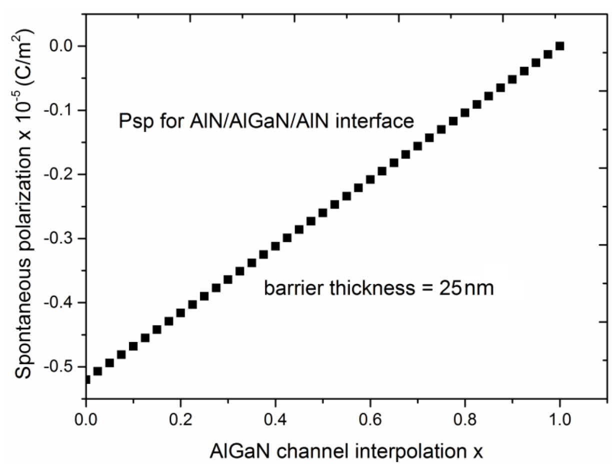

Figure 2. Spontaneous polarization for $AlN/Al_xGa_{1-x}N/AlN$ HEMT devices with x varied from 1 to 0.

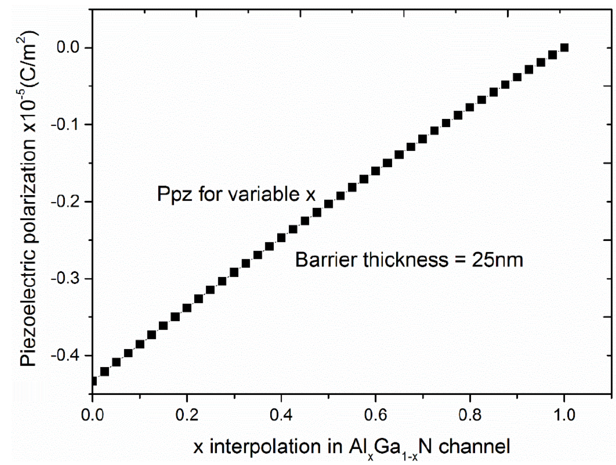

Figure 3. Piezoelectric polarization calculated for $AlN/Al_xGa_{1-x}N/AlN$ HEMT devices with x varied from 1 to 0.

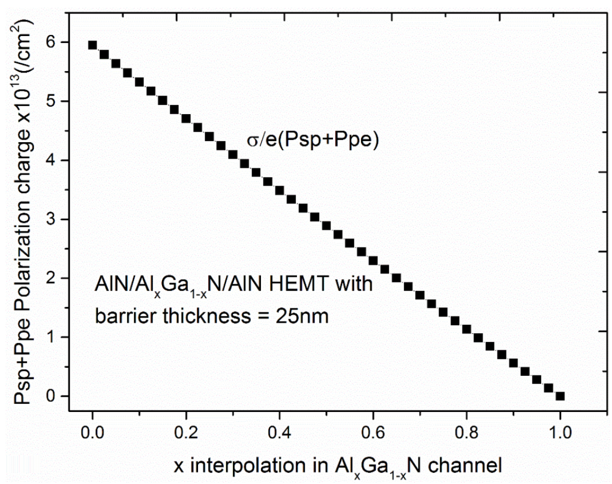

Figure 4. Total polarization charge using spontaneous and piezoelectric polarization with the electron charge calculated for a barrier thickness of 25 nm.

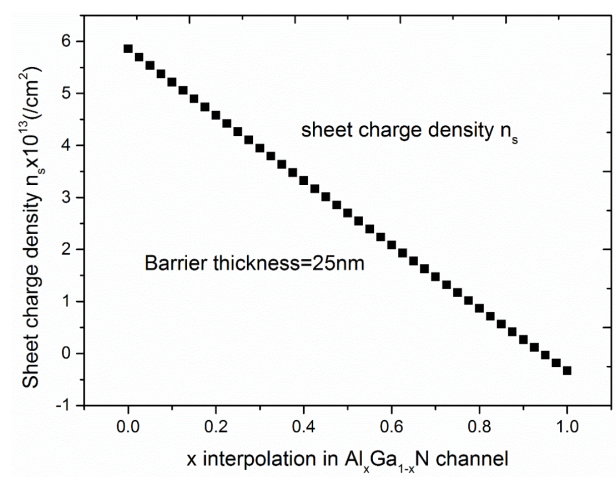

Figure 5. Sheet carrier density calculated with a barrier thickness of 25 nm for AlN-to-GaN channel region.

In Figure 6, constant partial strain relaxation is assumed as 0.5 in the channel, with a constant interpolation x of 0.51. For a barrier thickness of 25 nm, the sheet charge density reported is $2.6407 \times 10^{13}/cm^2$. This result is consistent with experimentally reported carrier density of $2.8 \times 10^{13}/cm^2$ [12]. Constant x interpolation is assumed from the experimental literature.

When strain relaxation is 0.45 in Eq. (7), the carrier density is $2.7648 \times 10^{13}/cm^2$ (Figure 7). This carrier sheet charge density is well matched with experimentally reported data. According to these results, AlN is partially strain-relaxed with the AlGaN channel, using the AlN buffer region [12]. A constant strain relaxation of 0.45 is included here. Nickel (Ni) gate metal is employed for better channel control and to reduce contact resistance. The drain current versus transconductance of the investigated device is obtained by simulations using the Sentaurus TCAD device simulator (Synopsys). A transconductance of 575 mS/mm is obtained in the above device with variable gate voltage (Figure 8). The maximum drain current reported in this device is 600 mA/mm. However, the performance of the device is limited due to increased surface defects and short channel effects.

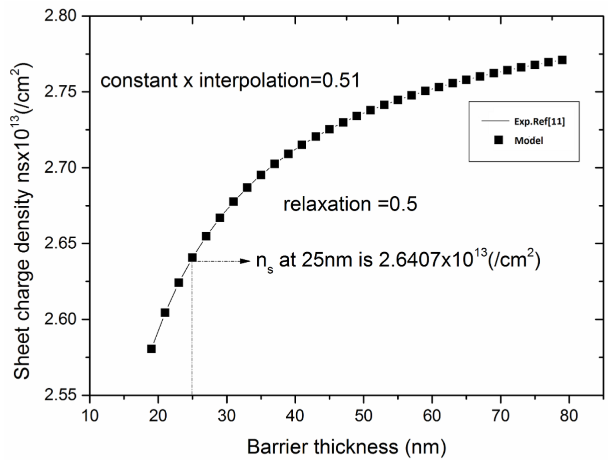

Figure 6. Sheet charge density versus barrier thickness for a constant $x = 0.51$ as calculated from the experimental literature [12]. A constant strain relaxation of 0.5 is taken into account here.

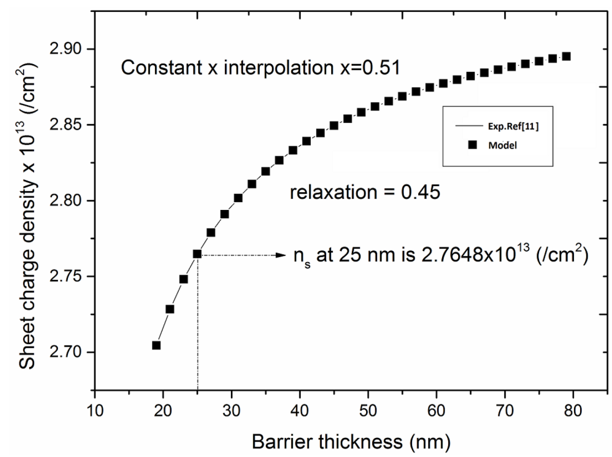

Figure 7. Carrier density for a constant $x = 0.51$ as calculated from the experimental literature [12].

The device is characterized by fixing the Al content in the AlGaN/AlN interface. Higher Al content ($x = 0.51$) of the device represents the normally OFF behavior of AlGaN/AlN-based devices (Figure 9). The resultant carrier concentration is drastically reduced due to larger surface states in the AlN barrier. Passivation of the AlN barrier increases the carrier concentration due to reduction in surface state existence.

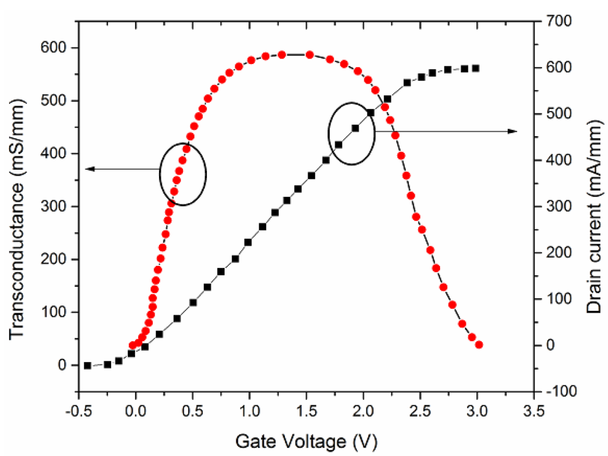

Figure 8. Effect of maximum transconductance and maximum drain current with respect to gate voltage sweep.

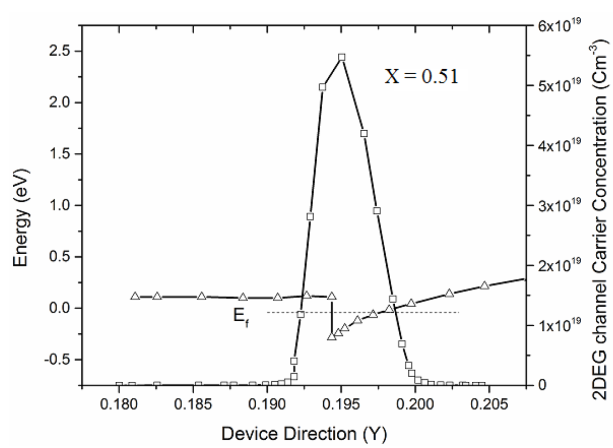

Figure 9. Increment of E_f (Fermi energy level) by varying Al% in the channel with two-dimensional electron gas carrier concentrations.

The model is validated with experimental data represented in [11] and shows good agreement. The expressions used in the model are simple and provide enough insight for exploring sheet carrier concentration density n_s for a novel AlGaN channel with AlN-barrier–based high-power and high-breakdown HEMT devices.

7. Conclusion

In this paper, the sheet carrier density model for various alloy compositions in an AlGaN channel with the AlN barrier on the performance of AlN/$Al_xGa_{1-x}N$/AlN HEMT has been analyzed. The AlN/$Al_xGa_{1-x}N$/AlN HEMT is modeled using spontaneous and piezoelectric polarization in all x interpolation. The carrier density with relaxation rate is also incorporated in polarization. The experimentally reported carrier density of 2.8 $\times$ $10^{13}/cm^2$ for device combination AlN/$Al_{0.51}Ga_{0.49}N$/AlN HEMT is well matched with our model predicting the partial strain relaxation for x = 0.45. If the strain relaxation is above 0.5, the carrier density is severely degraded. The degree of relaxation is varied from AlN to GaN in the channel. It shows that the AlN barrier with AlN buffer devices provide better relaxation than AlGaN channel devices.

References

[1] Hikita M, Yanagihara M, Nakazawa K, Ueno H, Hirose Y, Ueda T, Uemoto Y, Tanaka T, Ueda D, Egawa T. AlGaN/GaN power HFET on silicon substrate with source - via grounding (SVG) structure. IEEE T Elect Dev 2005; 52: 1963-1968.

[2] Chung JW, Hoke WF, Chumbes EM, Palacios T. AlGaN/GaN HEMT with 300 GHz fmax. IEEE Elect Dev Lett 2010; 31: 195.

[3] Ohno Y, Kuzuhara M. Application of GaN-based heterojunction FETs for advanced wireless communication. IEEE T Elect Dev 2001; 48: 517-523.

[4] Wu YF, Saxler A, Moore M, Smith RP, Sheppard S, Chavarkar PM, Wisleder T, Mishra UK, Parikh P. 30 W/mm GaN HEMTs by field plate optimization. IEEE Elect Dev Lett 2004; 25: 117-119.

[5] Nanjo T, Takeuchi M, Suita M, Oishi T, Abe Y, Tokuda Y, Aoyagi Y. Remarkable breakdown voltage enhancement in AlGaN channel high electron mobility transistors. Appl Phys Lett 2008; 92: 263-502.

[6] Tokuda H, Hatano M, Yafune N, Hashimoto S, Akita K, Yamamoto Y, Kuzuhara M. High Al composition AlGaN-channel high-electron–mobility transistor on AlN substrate. Appl Phys Express 3 2010: 121003.

[7] Yafune N, Hashimoto S, Akita K, Yamamoto Y, Tokuda H, Kuzuhara M. AlN/AlGaN HEMTs on AlN substrate for stable high-temperature operation. IEEE Elect Device Lett 2014; 50: 211-212.

[8] Raman A, Dasgupta S, Rajan S, Speck JS, Mishira UK. AlGaN channel high electron mobility transistors: Device performance and power-switching figures of merit. Jap J Appl Phys 2008; 47: 3359-3361.

[9] Satoh I, Arakawa S, Tanizaki K, Miyanaga M, Yamamoto Y. Sublimation growth of nonpolar AlN single crystals and defect characterization. Phy Stat Solidi 2010; 7: 1767-1769.

[10] Herwig H, Reuters B, Kalisch H, Vescan A. AlN barrier HFETs with AlGaN channels to shift the threshold voltage to higher positive values: a proposal. Semicond Sci Tech 2013; 28: 074017.

[11] Ambacher O, Smart J, Shealy JR, Weimann NG, Chu K, Murphy M, Schaff WJ, Eastman LF. Two-dimensional electron gases induced by spontaneous and piezoelectric polarization charges in N- and Ga-face AlGaN/GaN heterostructures. J App Phys 1999; 85: 3222-3233.

[12] Hashimoto S, Akita K, Yamamoto Y, Ueno M, Nakamura T, Takeda K, Iwaya M, Honda Y, Amano H. Enhancement of two-dimensional electron gases in AlGaN-channel high-electron–mobility transistors with AlN barrier layers. Phy Stat Solidi 2012; 209: 501-504.